ORIGINAL SCIENTIFIC PAPER OPEN ACCESS

CFD simulation of heat transfer in a combustion chamber

Đorđe Novčić[1*], Rade Karamarković[1] , Miloš Nikolić[1]

[1] University of Kragujevac, Faculty of Mechanical and Civil Engineering, Kraljevo, Serbia

ARTICLE INFO

[*] **Correspondence:** novcic.d@mfkv.kg.ac.rs

DOI: 10.5937/engtoday2600007N

UDC: 621(497.11) **ISSN:** 2812 – 9474

Article history: Received 15 January 2026; Revised 20 February 2026; Accepted 28 February 2026

ABSTRACT

Solid biomass represents the most important renewable energy source in the Republic of Serbia; however, its combustion in small-scale boilers is often associated with increased pollutant emissions. This study examines the influence of refractory elements on heat transfer in the combustion chamber of wood-log gasification boiler. These elements play a crucial role in multistage combustion systems, especially for moist biomass, by enhancing radiative and convective heat transfer, promoting more complete combustion, and reducing gaseous and particulate emissions while minimizing material usage. Special attention is given to the CFD optimization of the refractory ceramic length and the position of the producer gas inlet within the combustion chamber. Non-premixed combustion was modeled by solving the energy equation, applying the standard k–ε turbulence model and the DO radiation model. The results demonstrate that the most effective configuration employs a refractory element that creates a U-shaped flow path, which extends the residence time of flue gases in the chamber. Achieving this flow path requires the element to be at least one half to two thirds the length of the chamber, thereby positioning the combustion zone of the producer gas above the flue gas outlet.

KEYWORDS

Biomass, Wood, Flue gas, CFD, Combustion chamber.

1. INTRODUCTION

The Energy Strategy of the Republic of Serbia, along with the ongoing energy crisis, provides a strong impetus for intensified utilization and research of renewable energy sources [1]. Among these, solid biomass represent the most significant renewable energy resource in the Republic of Serbia [2]. Although wood has been used as a fuel since the earliest stages of human civilization, considerable potential for technical improvements in its combustion processes still exists [3]. Despite being a renewable energy source, wood combustion results in the emission of substantial quantities of pollutants into the atmosphere [4,5]. The scale and importance of these emissions are particularly evident in the elevated concentrations of various pollutants recorded in urban areas with a high density of individual heating systems across many cities in the Republic of Serbia [6]. This paper investigates how additional design measures can simultaneously improve heat transfer, achieve more complete combustion, suppress pollutant formation, and reduce emissions from solid biomass boilers. In order to decrease material consumption and emissions from these boilers, both primary [7] and secondary [8,9] measures are employed. Primary measures encompass technical solutions aimed at achieving complete combustion and preventing particulate matter emissions through the implementation of structural elements within the boiler itself. The paper places emphasis on the most efficient utilization of refractory elements in the combustion chambers of solid biomass boilers. These elements are applied in systems with multistage combustion, particularly in the combustion of moist biomass, and serve multiple functions: they reduce the

dimensions of the zone in which heat is primarily transferred by radiation (thereby reducing material usage and, consequently, the final cost of the boiler), enable more complete combustion, enhance heat transfer, and contribute to the reduction of gaseous pollutant emissions as well as particulate matter. The aim of this paper was to determine the optimal size of the refractory ceramic and the optimal position of the producer gas inlet into the combustion chamber. In the literature, there are several classifications of refractory elements; hence, no single unifed classification exists. Based on their form, refractory materials are divided into shaped refractory bricks and unshaped (monolithic) materials, such as refractory concretes [10]. The most commonly used refractory brick shapes are shown in Fig. 1. Among various shapes, a standard rectangular refractory brick was selected for this study due to its simplicity and common use [10].

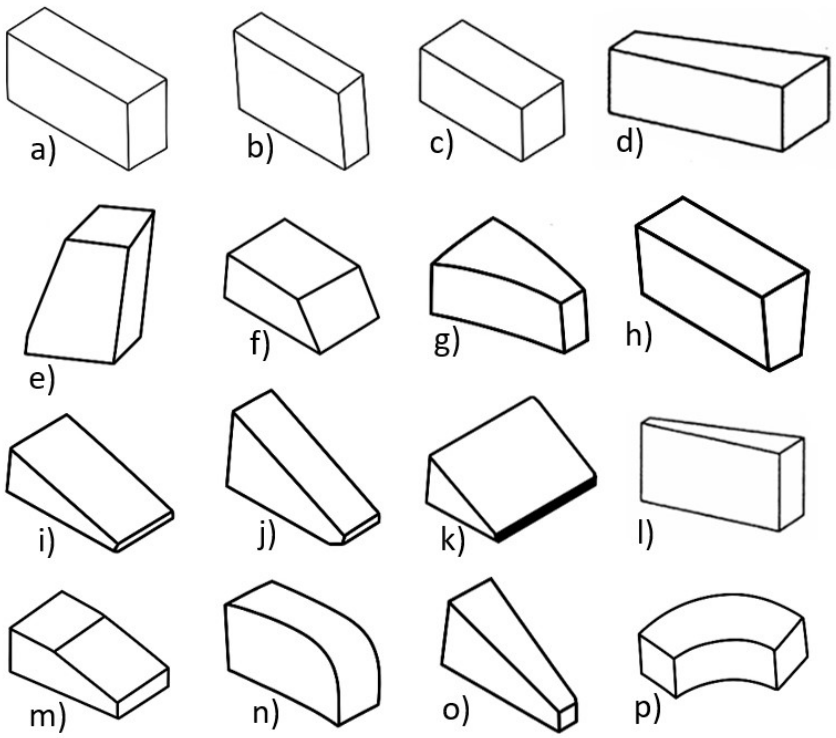

Figure 1: The most commonly used refractory brick shapes. a – straight, b - split, c – soap or closer, d – key brick, e – skew back, f – end skew on flat, g – end arch, h – side arch, i – feather end, j - feather end on edge, k – feather side, l – wedge, m – bevel brick, n – bullnose or jamb brick, o – dome brick, p – circle brick. [10,11]

2. THE CFD MODEL

A commercially available software ANSYS, together with its FLUENT 18.1 module, was employed to perform numerical simulations of producer gas combustion within the combustion chamber. The simulations were performed based on the defined geometry, generated computational mesh, and boundary conditions. In the development of the Non-premixed combustion model, the energy equation was solved, the standard k–ε turbulence model was adopted, and the Discrete Ordinates radiation model was applied. For radiation modeling, the wsggm-domain-based approach was used to determine the absorption coefficient. Figure 2a shows the 3D model of the proposed combustion chamber design of wood-log gasification boiler.

2.1. Mesh details

Figure 2b shows the computational mesh, represented by a cross-section of the combustion chamber. The mesh consists of 33064 nodes and 168327 elements. The minimum and maximum element side lengths are 0.545 mm and 20 mm, respectively. The mesh quality is considered satisfactory, as the average values of element quality, aspect ratio, orthogonal quality, and skewness fall within acceptable limits, amounting to 0.773, 2.21, 0.691, and 0.307, respectively [12].

2.2. Boundary conditions

The producer gas inlet (0.00373 kg/s, 497°C) to the combustion chamber was defined as a mass flow inlet with a uniform distribution over the cross-section (1 in Fig. 2). Combustion air (0.00713 kg/s, 300°C) was supplied through two inlet locations, both modeled as mass flow inlets with uniformly distributed flow (2 in Fig. 2). The flue gas outlet, corresponding to the inlet of the tubular heat exchanger (6 in Fig. 2), was specified as a pressure outlet with a relative static pressure of 0 Pa. Similarly, the boiler water inlet (0.2 kg/s, 55°C) was defined as a mass flow inlet with uniform

distribution (8 in Fig. 2), while the water outlet was modeled as a pressure outlet with a relative pressure of 0 Pa (9 in Fig. 2). All remaining surfaces were defined as wall boundary conditions. The parameters used in the numerical simulations for the refractory ceramics (corundum 90) were taken from [13] and are as follows: λ=2.33 W/mK, C_p=1.118 kJ/kgK, and ρ=2.83 g/cm3. Table 1 presents the composition of producer gas used in the numerical simulations.

Table 1: Producer gas composition used in the numerical simulations.

CO %	CO_2 %	CH_4 %	H_2 %	H_2O %	N_2 %	O_2 %	C_7H_{16} %
2.344	19.043	0.293	0.195	21.484	53.906	0.293	2.442

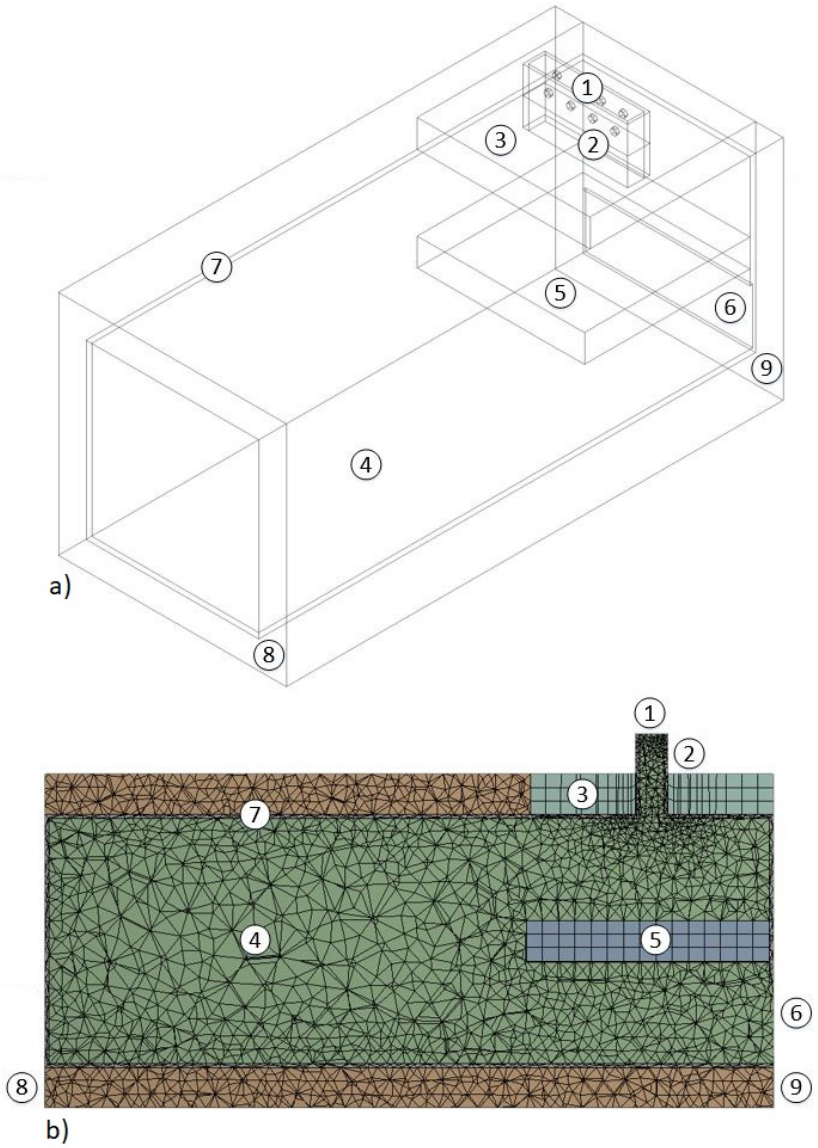

Figure 2: a - 3D model of the combustion chamber design of wood log gasification boiler, b – the computational mesh represented by a cross-section of the combustion chamber. 1 – producer gas inlet, 2 – combustion air inlet, 3 – refractory ceramics separating the gasification from the combustion chamber, 4 – combustion chamber, 5 – refractory ceramics inside the combustion chamber, 6 – flue gas outlet, 7 – boiler steel plate, 8 - boiler water inlet, 9 - boiler water outlet.

2.3. Effect of refractory length and gas inlet position on heat transfer

A total of 25 configurations were analyzed, combining five different lengths of the refractory ceramic with five positions of the producer gas inlet, as listed in Tab. 2. The producer gas inlet position is denoted by *x*, and the refractory ceramic length by *y*. Each configuration is labeled as x_iy_i, with the index *i* ranging from 1 to 5, starting from x_1y_1 up to x_5y_5.

Table 2: Configurations x_iy_i used in the numerical simulations.

Producer gas inlet position (x_i)	Refractory ceramic length (y_i)
x_1=150 mm	y_1=300 mm

Producer gas inlet position (x_i)	Refractory ceramic length (y_i)
x_2=250 mm	y_2=375 mm
x_3=350 mm	y_3=450 mm
x_4=450 mm	y_4=525 mm
x_5=550 mm	y_5=600 mm

Figure 3 shows the CFD model of the combustion chamber.

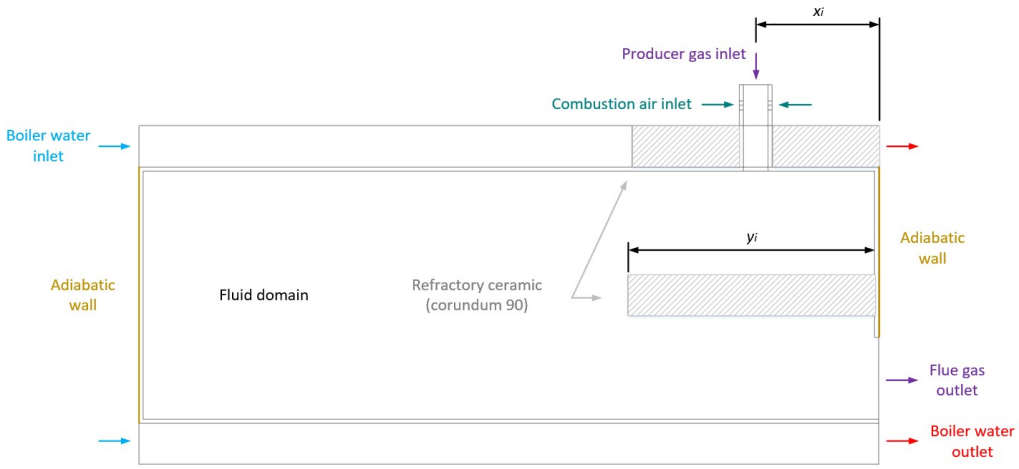

Figure 3: CFD model of the combustion chamber.

3. RESULTS

The results of the numerical simulations are presented in Fig. 4. The convergence criterion (< 1×10^{-4}) was achieved just before the 13000th iteration, corresponding to a total computational time of approximately 35 minutes. In Fig. 4, the total heat transfer from the flue gas to the boiler water obtained from the CFD simulations is depicted by the black line, while the total energy brought in the combustion chamber is shown by the red dashed-dotted line. The analysis reveals that the most favorable heat transfer performance is achieved when the producer gas inlet is positioned closest to the flue gas outlet and the refractory ceramic length is at least half the combustion chamber length. Specifically, configurations x_1y_3, x_1y_4, and x_1y_5 (highlighted in gold) demonstrate this optimal geometry. In these cases, the extended refractory element creates a longer flow path, thereby increasing the residence time of the flue gases and enhancing heat transfer. The total heat transfer for these optimal configurations shows minimal variation, ranging from 13.33 to 13.5 kW. Conversely, the least favorable performance is observed when the producer gas inlet is positioned near the boiler water inlet, as seen in configurations x_3y_1, x_3y_2, and x_4y_3 (highlighted in green). In these arrangements, heat transfer is significantly reduced, with values varying only slightly between 10.91 and 10.99 kW. Overall, the difference between the most and least favorable configurations is approximately 2.5 kW.

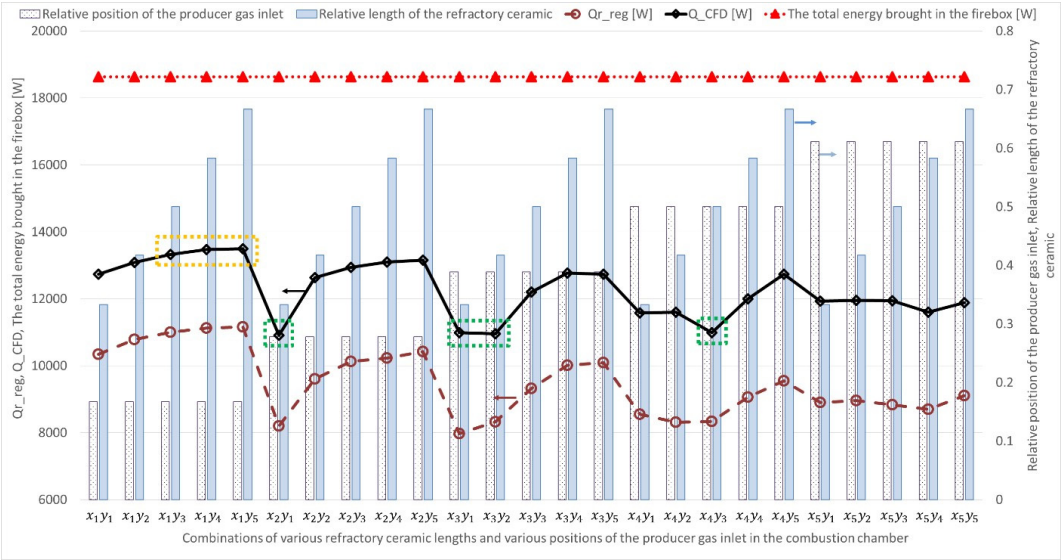

Figure 4: Results of CFD simulations.

In Fig. 4, radiative heat transfer from the flue gas to the boiler water is shown by the dark red dashed line. Regression analysis was used to derive the following mathematical equation (in watts) describing this process:

$$Q_{r\_reg} = c_0 + c_1 p_r + c_2 l_r + c_3 (p_r / l_r)^2 + c_4 (\Delta T_{gas} / \Delta T_{water})^2 + c_5 (\Delta T_{gas} - \Delta T_{water})^2 + c_6 (T_{gas_{mean}} / T_{water_{mean}})^2 + c_7 (p_r / l_r)^3 + c_8 (\Delta T_{gas} / \Delta T_{water})^3 + c_9 (T_{gas_{mean}} / T_{water_{mean}})^3 + c_{10} (p_r / l_r)^4 + c_{11} (\Delta T_{gas} / \Delta T_{water})^4 + c_{12} (T_{gas_{mean}} / T_{water_{mean}})^4 \quad (1)$$

Where c_i are constants (Tab. 3), $p_r=p_r/L$ and $l_r=l_r/L$ denote the relative inlet position and refractory length, respectively, with L=900 mm. ΔT_{gas} and ΔT_{water} are the gas and water inlet–outlet temperature differences, and T_{gas_mean} and T_{water_mean} are the corresponding mean temperatures.

Table 3: Constants used in (1)

c_0	c_1	c_2	c_3	c_4	c_5	c_6	c_7	c_8	c_9	c_{10}	c_{11}	c_{12}
322835	3644.1	-399.7	-8198.9	15.6	0.22	-267997.9	8131.5	-26.1	133772.7	-2197.2	3.5	-18662.9

Configuration p_1l_3 was selected as optimal, as it achieves near-maximal heat transfer performance while employing a shorter refractory length, thereby offering a favorable balance between efficiency and material economy. The numerical results for this configuration are shown in Fig. 5a. The flue gas temperature field indicates outlet temperatures between 425 and 549°C, confirming that the extended flow path, and correspondingly increased flue gas residence time, significantly enhances heat transfer. Although the primary role of the refractory ceramic is to separate the gas inlet from the outlet, positioning it closer to the outlet enhances convective heat transfer and promotes radiative heat exchange from hotter to cooler regions. The simulations also indicate an average water temperature rise of 9-20°C during heat exchange. Conversely, Fig. 5b presents configuration p_4l_3, which exhibits unfavorable heat transfer characteristics, with clearly visible colder zones caused by the more distant producer gas inlet position.

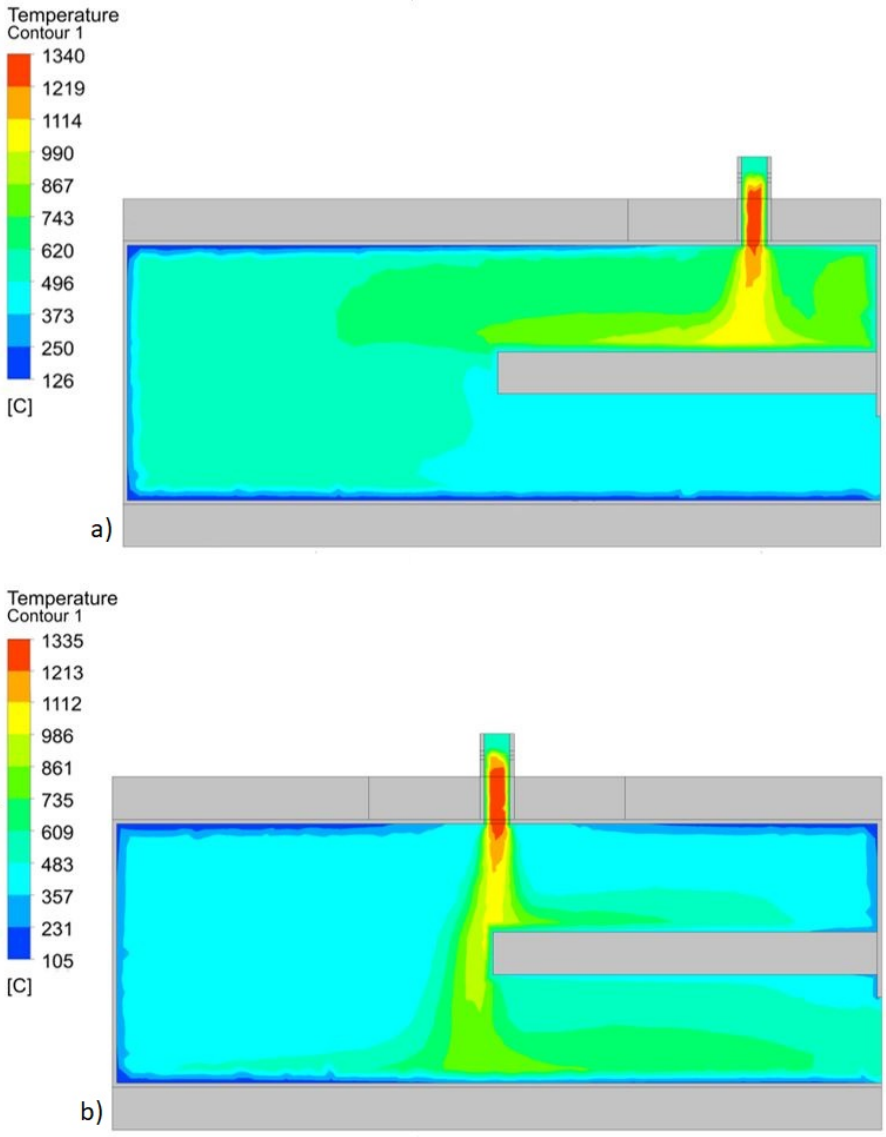

Figure 5: Results of CFD simulations. a - the optimal configuration p_1l_3, b - the least favorable configuration p_4l_3.

4. CONCLUSIONS

This paper investigates how the geometry and placement of refractory ceramics influence heat transfer and combustion performance in wood-log gasification boilers. The results shows that refractory ceramics in wood-log gasification boilers should be treated as flow-shaping and radiative elements rather than merely as thermal protection. By controlling the residence time, flow topology, and exposure of hot gas to radiative surfaces, the refractory layout governs the dominant heat-transfer mechanisms inside the combustion chamber.

The CFD simulations shows that the most effective configurations create a U-shaped flow path that separates the gas inlet from the outlet and extends the flue-gas residence time. A refractory length of approximately one half to two thirds of the chamber length is sufficient to achieve this effect. Positioning the ceramic closer to the gas outlet promotes heat transfer by directing radiative and convective fluxes from hotter to cooler regions.

ACKNOWLEDGEMENTS

This research was supported by the Science Fund of the Republic of Serbia, #GRANT No 5959, Active condensation hybrid systems in biomass combustion, AC-BC.

REFERENCES

[1] J. Kisin, J. Ignjatović, and A. Mashovic, "Energy crisis in Serbia: causes, effects, government response and potential for sustainable development", Proceedings of the 10th International Scientific Conference on Climate Change, Economic Development, Environment and People (CCEDEP), Travnik (Bosnia and Herzegovina), pp. 86-102, (2023)

[2] Ministarstvo rudarstva i energetike Republike Srbije, "Strategija razvoja energetike Republike Srbije do 2025. godine sa projekcijama do 2030. godine", https://arhiva.mre.gov.rs/latinica/dokumenta-efikasnost-izvori.php

[3] R. Karamarković, "Metode transformacije energije", Fakultet za mašinstvo i građevinarstvo u Kraljevu, Kraljevo (Srbija), (2022)

[4] H. A. C. Denier Van Der Gon, R. Bergström, C. Fountoukis, C. Johansson, S. N. Pandis, D. Simpson, and A. J. H. Visschedijk, "Particulate emissions from residential wood combustion in Europe - revised estimates and an evaluation", Atmospheric Chemistry and Physics, Vol. 15(11), p. 6503–6519, https://doi.org/10.5194/acp-15-6503-2015, (2015)

[5] A. Cincinelli, C. Guerranti, T. Martellini, and R. Scodellini, "Residential wood combustion and its impact on urban air quality in Europe", Curr. Opin. Environ. Sci. Heal., Vol. 8, p. 10–14, https://doi.org/10.1016/j.coesh.2018.12.007, (2019)

[6] Agencija za zaštitu životne sredine (SEPA), "Godišnji izveštaj o stanju kvaliteta vazduha u Republici Srbiji 2023. Godine", https://sepa.gov.rs/wp-content/uploads/2024/10/Vazduh2023.pdf

[7] T. Nussbaumer, "Combustion and Co-combustion of Biomass: Fundamentals, Technologies, and Primary Measures for Emission Reduction", Energy & Fuels, Vol. 17(6), p. 1510–1521, https://doi.org/10.1021/ef030031q, (2003)

[8] R. Singh and A. Shukla, "A review on methods of flue gas cleaning from combustion of biomass," Renewable and Sustainable Energy Reviews, Vol. 29, p. 854–864, https://doi.org/10.1016/j.rser.2013.09.005, (2014)

[9] O. Sippula, J. Hokkinen, H. Puustinen, P. Yli-Pirilä, and J. Jokiniemi, "Particle emissions from small wood-fired district heating units," Energy & Fuels, Vol. 23(6), p. 2974–2982, https://doi.org/10.1021/ef900098v, (2009)

[10] P. Sengupta, "Refractories for the Chemical Industries", Springer International Publishing, Cham (Switzerland), (2020)

[11] Harbison-Walker, "Harbison-Walker Handbook of Refractory Practice", Harbison-Walker Refractories Company, Moon Township, PA, https://www.mha-net.org/docs/Harbison%20Walker%202005%20Handbook.pdf

[12] https://www.mechead.com/mesh-quality-checking-ansys-workbench/

[13] A. Osterode, "D6 Properties of Solids and Solid Materials", Springer-Verlag, Berlin (Germany), (2010)